Determining the Origin of Ultrahigh-Pressure Lherzolites

The occurrence of coesite and diamond in regional ultrahigh-pressure metamorphic rocks requires that rocks formed at pressures of 3 to 4 GPa (100 to 120 km below the Earth's surface) have been transported back to the surface (*1*). L. Dobrzhinetskaya *et al.* suggest that garnet lherzolite from the Alpe Arami massif of the Central Alps may have been metamorphosed at much higher pressures of 10 to 15 GPa (at a depth of 300 to 450 km) (*2*), which would imply that pieces of the mantle transition zone can be transported to the Earth's surface by as yet unknown tectonic processes (*3*).

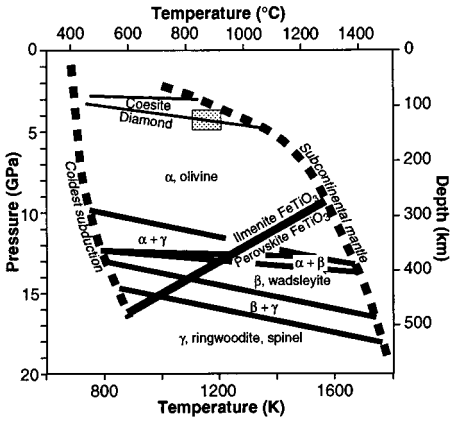

Fig. 1. Pressure-temperature stability fields for $Mg_{1.8}Fe_{0.2}SiO_4$ (*23*) and $FeTiO_3$ (*24*). Conditions within the upper mantle range from the coldest subducting lithosphere to the subcontinental upper mantle, as shown by dotted lines (*25*). Box shows equilibrium pressure and temperature of silicate minerals in Chinese garnet lherzolite SL14a.

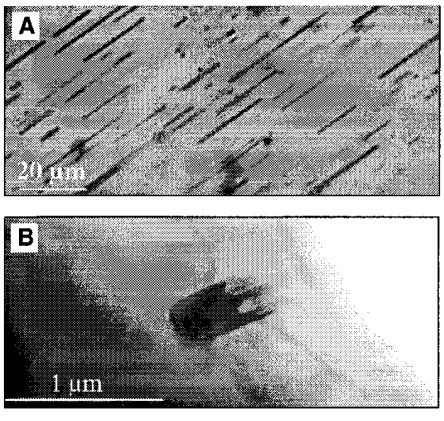

Fig. 2. Olivine from ultrahigh-pressure garnet lherzolite near the town of Chijiadian in the Sulu area of China. (**A**) Transmitted light optical photomicrograph showing $FeTiO_3$ rods within $Mg_{1.8}Fe_{0.2}SiO_4$ olivine. (**B**) Transmission electron micrograph of an (010) section of a single titanate rod.

Dobrzhinetskaya *et al.* interpreted Alpe Arami as a piece of the mantle transition zone on the basis of the discovery of (i) micrometer-scale $FeTiO_3$ rods in olivine, (ii) a distinct lattice preferred orientation of olivine, and (iii) high inferred TiO_2 contents of olivine (*2*). Transmission-electron microscopy revealed that the titanate rods were topotactic with the host olivine, parallel the [010] direction of olivine, and had four structures: ilmenite, and three previously unrecognized crystal structures interpreted as intermediate between ilmenite and the denser perovskite structure of $FeTiO_3$ (*2*). Because all other reported $FeTiO_3$ inclusions in olivine are plates of ilmenite structure (*4*), the rods in Alpe Arami olivine were distinctive and hypothesized to have exsolved at 10 to 15 GPa (*5*) (300 to 450 km) as perovskite, followed by variable conversion to ilmenite (Fig. 1) (*2*). Pressures of 10 to 15 GPa are high enough that the Alpe Arami olivine could have been in the more dense wadsleyite (modified spinel) or ringwoodite (spinel) structure. In support of this possibility, Green and Dobrzhinetskaya (*6*) have noted that the distinct lattice preferred orientation of Alpe Arami olivine may have formed when wadsleyite or ringwoodite were stable.

The strongest argument Dobrzhinetskaya *et al.* make in support of the statement that Alpe Arami came from the transition zone is that the titanate "inclusions constitute generally more than 1%, and locally as much as 3% by volume, of the olivine crystals." This argument implies that "prior to exsolution the olivine contained about 0.7 wt% TiO_2 (locally perhaps as much as 2 wt% TiO_2)" (*2, 7*). TiO_2 contents of analyzed olivines from all other garnet lherzolites are much lower. Kimberlitic garnet lherzolite xenoliths, some of which originated as deep as 400 to 500 km (*8*), have olivine grains that contain, on average, 220 ± 110 ppm, and never more than 600 ppm TiO_2 (*9*). The tremendously higher Ti contents inferred for Alpe Arami olivine led Dobrzhinetskaya *et al.* to propose that the $(Mg,Fe)_2SiO_4$ phase must have been a higher pressure mineral such as wadsleyite and ringwoodite, which have high Ti solubility, before its transformation to olivine, which has low Ti solubility (*2*).

In searching our own collections of ultrahigh-pressure lherzolites for olivine crystals containing titanate rods, we discovered an occurrence of such rods in olivine (Fig. 2) from the Chijiadian garnet lherzolite, which crops out in the Sulu area of eastern China. The Sulu area contains widespread ultrahigh-pressure regional metamorphic rocks (*10, 11*), which, including the Chijiadian lherzolite, experienced metamorphic pressures of at least 3 GPa, as indicated by the presence of coesite in eclogite included within the lherzolite (*10*). The composition of peak metamorphic silicate minerals in the Chijiadian lherzolite (Table 1) give no indication of transition zone pressures: Al partitioning between enstatite and garnet indicates pressures of 4.1 ± 0.6 GPa, and the distribution of Ca between olivine and diopside suggests equilibration at ~4.4 GPa (*12*). Fe-Mg partitioning among garnet, enstatite and diopside indicates a temperature of ~875° ± 50°C (*13*). Thermobarometric measurements indicate similar maximum pressures, 3 to 5 GPa, for the Alpe Arami massif (*14*).

Olivine grains in the Chijiadian lherzolite contain rod-like inclusions (Fig. 2) of the composition $Fe_{0.82}Mg_{0.15}M_{0.03}$ TiO_3 (Table 1)—more magnesian than is present in the Alpe Arami titanates, which are $Fe_{0.94}Mg_{0.06}TiO_3$ (*2*). The rods have two dimensions of 0.2 to 0.5 μm, whereas the third dimension is typically ~20 μm. This is smaller than the 0.2 to 4 μm diameter Alpe Arami rods, which are also more densely packed (*2*). Like Alpe Arami, inclusions in the Chijiadian olivines we have imaged with transmission electron microscopy have long axes that parallel the [010] direction of the host olivine crystals. Significantly, the titanate rods at Alpe Arami are not an isolated occurrence.

We measured the TiO_2 content of Chijiadian and Alpe Arami olivines directly by electron probe microanalysis and secondary

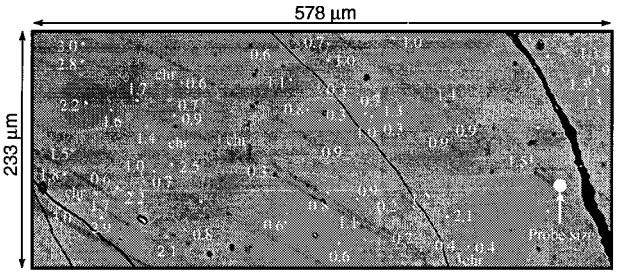

Fig. 3. Back-scattered electron image of olivine grain "ol-1" from Alpe Arami garnet lherzolite 3-73-AA of (*2*); bright spots are titanate and chromite ("chr") inclusions. Numbers show wt% TiO_2 measured with nominally 5-μm diameter electron beams.

ion mass spectrometry. The bulk TiO_2 contents of individual olivine grains from both localities were analyzed with a comprehensive grid of 5-, 10-, and 20-μm diameter electron beams at 15 kV accelerating voltage, 15 to 100 nA sample current, and counting times of 200 to 2000 seconds (Table 1). All analyzed grains yielded bulk TiO_2 contents of hundreds of parts per million (*15*), including three inclusion-rich grains, "ol-1," "ol-2," and "ol-3" from sample 3-73-AA, loaned to us by L. Dobrzhinetskaya. To pursue this factor of 10 or more disparity between our measured TiO_2 contents and their calculated TiO_2 contents, we isolated an area of 225 × 575 μm from grain "ol-1" to analyze in greater detail (Fig. 3). With the use of a nominal 5-μm diameter electron beam, we analyzed every inclusion visible with backscattered electrons. If this grain contained 0.5-vol% rods that are 1, 2, or 4 μm in diameter (*16*), there must be 825, 205, or 51 rods, respectively, within this 129,375-μm^2 area. There are only 71 titanate inclusions visible with back-scattered electrons. Assuming that the rods are pure $FeTiO_3$ and that our nominal 5-μm electron beam excited x-rays within a 7-μm diameter volume, our individual spot analyses, which average 1.3 ± 0.9 wt% TiO_2, indicate an average rod diameter of 1.2 ± 0.8 μm. From 71 1.2-μm diameter rods in an area of 129,375 μm^2, we compute a bulk TiO_2 content of 329 ppm, in agreement with our broad-beam analyses. We conclude that the TiO_2 contents of Alpe Arami olivines are not 7600 to 23,000 ppm (*1*), but within the range of values reported from worldwide garnet lherzolite xenoliths (*9*) and cannot be used to argue that Alpe Arami had its origin in the mantle transition zone.

The second strongest argument made by Dobrzhinetskaya *et al.* for an ultradeep origin for Alpe Arami is that some titanate rods have previously unrecognized crystal structures. Their descriptions of the new polymorphs of $FeTiO_3$ were based on electron diffraction data [figure 3 of (*2*)]. However, the diffraction patterns of $FeTiO_3$ and olivine seen in this figure can be explained by dynamical diffraction between overlapping olivine and ilmenite structures, without requiring novel $FeTiO_3$ structures (*17*). Because electrons are dynamically diffracted, forbidden reflections are common in electron diffraction patterns (*18*). Moreover, if the structures of an inclusion and its host overlap in the direction of the zone axis used for the diffraction pattern, reflections from one structure can be rediffracted by the other, resulting in a complex pattern with a periodicity that reflects both structures (*19*).

The diffraction pattern in figure 3C of the report (*2*) results from the following orientation relation between olivine and ilmenite: $[100]_{ol} \parallel [0001]_{ilm}$, $[010]_{ol} \parallel \langle 11\bar{2}0\rangle_{ilm}$, and $[001] \parallel \langle 1\bar{1}00\rangle$ (Table 2) (*20*). This orientation relation and the diffraction symmetry of ilmenite and olivine also explain the features shown in figures 3A and 3B of the report (*2*) without the need to appeal to novel $FeTiO_3$ structures. In figure 3B of the report (*2*), the hexagonal diffraction pattern of the ilmenite [0001] zone is almost perfectly superimposed on the olivine [100] pattern because of the pseudo-hexagonal structure of the olivine (100) planes and the nearly identical d-spacings of coincident reflections (Fig. 4A). Similarly, figure 3A of the report (*2*) can be interpreted as the superposition of the olivine [001] and ilmenite $\langle 1\bar{1}00\rangle$ zone axes (Fig. 4B), which results in nearly identical d-spacings of coincident reflections (Table 2). The ilmenite (hki3l) reflections overlap the olivine (h4k0) reflections, resulting in the higher intensities that are visible in the pattern, and the small differences in d-spacings result in a slight splitting between the superimposed reflections.

Thus, if reflections from the ilmenite inclusion are rediffracted by the olivine host, dynamical diffraction distributes this slight splitting to all the olivine reflections, yielding an apparent second phase with nearly the same unit cell and diffraction symmetry as olivine. Without diffraction data from the pure $FeTiO_3$ inclusions, there is no compelling evidence for the presence

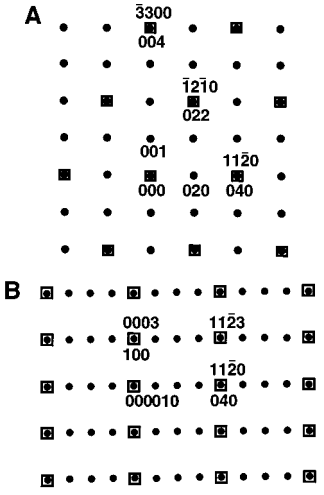

Fig. 4. Schematic electron diffraction patterns showing the superposition of (**A**) the ilmenite [0001] on the olivine [100] zone axes and (**B**) the ilmenite [01$\bar{1}$0] on the olivine [001] zone axes. Olivine reflections are filled circles labeled with three (hkl) indices, and ilmenite reflections are open squares labeled with four (hkil) indices. Streaking along a* and c* of olivine in the electron diffraction patterns of (*2*) can be explained by a slight mismatch of the two lattices along these directions with a nearly perfect match along the olivine b axis.

Table 1. Compositions of minerals in Chijiadian garnet lherzolite SL14a and Alpe Arami samples AA8 and 3-73-AA. Oxide concentrations with decimal points are wt%, numbers without are parts per million; secondary ion mass spectrometry analyses are italicized (*22*). Sample size of each mineral, (*n*). No data, n.d.

Analyses	Chijiadian lherzolite sample SL14a					AA8	3-73-AA
	Titanate (6)	Enstatite (92)	Diopside (116)	Garnet (83)	Olivine (271)	Olivine (964)	Olivine (973)
SiO_2	n.d.	57.87 ± 0.95	53.51 ± 1.46	41.77 ± 0.43	40.50 ± 0.42	40.70 ± 0.42	41.48 ± 0.39
TiO_2	52.5 ± 1.3	*300 ± 6*	*349 ± 162*	*250 ± 5*	269 ± 188/*100 ± 20*	205 ± 701	202 ± 305
Al_2O_3	n.d.	0.25 ± 0.10	1.29 ± 0.14	22.23 ± 0.23	*20*	n.d.	n.d.
Cr_2O_3	0.4 ± 0.2	750 ± 330	8780 ± 1230	1.65 ± 0.21	233 ± 202/*15 ± 3*	n.d.	n.d.
V_2O_3	n.d.	*20 ± 4*	*618 ± 163*	*198 ± 194*	*<3*		
FeO*	38.9 ± 0.9	5.89 ± 0.17	2.80 ± 0.28	11.22 ± 0.27	9.06 ± 0.28	10.23 ± 0.20	9.09 ± 0.16
NiO	n.d.	885 ± 120	511 ± 182	*<170*	3951 ± 98		3764 ± 164
MnO	2.7 ± 1.0	970 ± 320	549 ± 281	4880 ± 220	919 ± 363	1478 ± 419	870 ± 216
MgO	4.1 ± 1.2	35.63 ± 0.19	16.37 ± 0.77	18.32 ± 0.16	50.42 ± 1.1	48.41 ± 0.69	49.1 ± 0.58
CaO	n.d.	*1230 ± 20*	21.50 ± 0.95	4.04 ± 0.19	*100 ± 20*	n.d.	
Na_2O	n.d.	*70 ± 5*	1.68 ± 0.22	*<40*	*<40*	n.d.	
K_2O	n.d.	*<50*	*<50*	*<50*	<50		
Li_2O	n.d.	*<2*	*n.d.*	*<0.5*	*10*		
Sum	98.6 ± 0.9	99.98 ± 1.09	98.23 ± 0.28	99.92 ± 0.78	100.52 ± 0.67	99.51 ± 1.0	99.65 ± 1.0

Table 2. Coincident reflections and d-spacings for olivine and ilmenite.

Source	Olivine	Ilmenite
Figure 3A of (*2*)	[001] zone	⟨1100⟩ zone
	100 (4.76Å)	0003 (4.68Å)
	040 (2.55Å)	$11\bar{2}0$ (2.54Å)
	140 (2.25Å)	$11\bar{2}3$ (2.23Å)
Figure 3B of (*2*)	[100] zone	[0001] zone
	004 (1.50Å)	$\underline{3}300$ (1.47Å)
	022 (2.58Å)	$\bar{1}2\bar{1}0$ (2.54Å)
	040 (2.55Å)	$11\bar{2}0$ (2.54Å)
Figure 3C of (*2*)	[010] zone	⟨$11\bar{2}0$⟩ zone
	200 (2.37Å)	$000\bar{6}$ (2.35Å)
	004 (1.49Å)	$03\bar{3}0$ (1.47Å)

of high-pressure $FeTiO_3$ polymorphs other than ilmenite in the Alpe Arami samples.

Thus, we regard the hypothesis that Alpe Arami, and by inference also the Chijiadian lherzolite, formed at 10 to 15 GPa in the transition zone as less plausible than formation at 4 GPa. It *is* possible that the Chinese or Alpine lherzolites experienced maximum pressures greater than 4 to 5 GPa, but additional evidence, such as the discovery of TiO_2 with αPbO_2 structure (stable at 5 to 7 GPa), high-pressure C2/c clinoenstatite (6 GPa), or majorite garnet (7 GPa) (*21*) is required.

B. R. Hacker
Department of Geological Sciences, University of California, Santa Barbara, CA 93106–9630, USA
E-mail: hacker@magic.geol.uscb.edu
T. Sharp
Department of Geology, Arizona State University, Tempe, AZ 85287, USA
R. Y. Zhang
J. G. Liou
Department of Geological and Environmental Sciences, Stanford University, Stanford, CA 94305–2115, USA
R. L. Hervig
Center for Solid State Science, Arizona State University,

REFERENCES AND NOTES

1. D. C. Smith, *Nature* **310**, 641 (1984); C. Chopin, *Contrib. Mineral. Petrol.* **86**, 107 (1984); S. Xu *et al.*, *Science* **256**, 80 (1992); A. I. Okay, *Europ. J. Mineral.* **5**, 659 (1993). "Ultrahigh" is used to describe metamorphic pressures of ~2 to 4 GPa.
2. L. Dobrzhinetskaya, H. W. Green II, S. Wang, *Science* **271**, 1841 (1996).
3. Alpe Arami is a peridotite massif approximately 400 × 1100 m in outcrop, surrounded by less dense continental gneiss [J. R. Moeckel, *Leidse Geol. Meded.* **42**, 61 (1969)]. The mantle transition zone is that portion of the mantle at depths of 400 to 650 km where $(Mg,Fe)_2SiO_4$ olivine transforms to its denser polymorph wadsleyite and then ringwoodite. Pressures at the top of the transition zone are 10 to 13 GPa [M. Akaogi, E. Ito, A. Navrotsky, *J. Geophys. Res.* **94**, 15,671 (1992)].
4. M. R. Drury and H. L. M. van Roermund, *Geology* **16**, 1035 (1988); D. Moseley, *Am. Min.* **66**, 976 (1981).
5. A. Mehta, K. Leinenweber, A. Navrotsky, M. Akaogi, *Phys. Chem. Mineral.* **21**, 207 (1994).
6. H. W. Green II and L. Dobrzhinetskaya, *Eos* **75**, 651 (1994).
7. $FeTiO_3$ is ~52.6 wt% TiO_2, and the densities of $FeTiO_3$ ilmenite and $Mg_{1.8}Fe_{0.2}SiO_4$ olivine are 4.8 and 3.3 g/cm^3, respectively [J. R. Smyth and T. C. McCormick, in *Mineral Physics and Crystallography: A Handbook of Physical Constants*, T. J. Ahrens, Ed. (American Geophysical Union, Washington, DC, 1995), pp. 1–17)], thus 1 to 3 vol% $FeTiO_3$ implies that the Alpe Arami olivine crystals contain 0.76 to 2.3 wt% or 7600 to 23,000 ppm of TiO_2.
8. Xenoliths are fist-sized fragments of Earth's mantle carried rapidly to the surface in volcanic eruptions. The great depth of origin of kimberlitic lherzolite xenoliths is evident from textures that demonstrate the solubility of pyroxene in garnet [V. Sautter, S. E. Haggerty, S. Field, *Science* **252**, 827 (1991)]; S. E. Haggerty and V. Sautter, *ibid.* **248**, 993 (1990).
9. R. L. Hervig, J. V. Smith, J. B. Dawson, *Trans. Royal Soc. Edinburgh: Earth Sci.* **77**, 181 (1986); R. L. Hervig and J. V. Smith, *Contrib. Mineral. Petrol.* **81**, 184 (1982).
10. R. Y. Zhang, J. G. Liou, B. Cong, *J. Metamorph. Geol.* **12**, 169 (1994); N. Hiramatsu, S. Banno, T. Hirajima, B. Cong, *Island Arc* **4**, 324 (1995).
11. X. Wang and J. G. Liou, *Geology* **19**, 933 (1991); B. R. Hacker, X. Wang, E. A. Eide, L. Ratschbacher, in *Tectonic Evolution of Asia*, A. Yin and T. M. Harrison, Eds. (Cambridge Univ. Press, Cambridge, 1995); B. R. Hacker and Q. C. Wang, *Tectonics* **14**, 994 (1995); B. R. Hacker, L. Ratschbacher, L. Webb, S. Dong, *Geology* **23**, 743 (1995); J. G. Liou *et al.*, in *Tectonic Evolution of Asia*, A. Yin and T. M. Harrison, Eds. (Cambridge Univ. Press, Cambridge, 1995), pp. 345–370. The location of the Chijiadian lherzolite body was shown by Zhang *et al.* (*10*).
12. Cited barometers are from G. P. Brey and T. Koehler [*J. Petrol.* **31**, 1353 (1990)].
13. Temperature estimates are from the garnet-clinopyroxene thermometer of E. J. Krogh [*Contrib. Mineral. Petrol.* **99**, 44 (1988)] and the clinopyroxene-orthopyroxene thermometer of G. P. Brey and T. Koehler [*J. Petrol.* **31**, 1353 (1990)] and derived from compositions of mineral cores.
14. W. G. Ernst, *J. Petrol.* **18**, 371 (1978).
15. These TiO_2 values are semi-quantitative because of the inhomogeneous distribution of TiO_2 within the olivine and because some measured values are below detection; there likely are real differences in TiO_2 content among the grains that our technique is too insensitive to detect. The accuracy of these analyses may be assessed by the agreement between our electron-probe (350 ± 210 ppm) and secondary ion mass spectrometry (300 ± 6 ppm) determinations of TiO_2 in SL14a enstatite. Subsequently, A.-C. Risold, V. Trommsdorff, E. Reusser, and P. Ulmer (*Terra Nova 9*, Abstract Suppl. 1, in press) reported laser inductively coupled plasma mass spectrometry measurements indicating TiO_2 contents of Alpe Arami olivines of <400 ppm, and Y. Ogasawara, Y. Nakajima, and J. Liou (*ibid.*) showed TiO_2 contents in Sulu olivines of about 300 ppm.
16. L. Dobrzhinetskaya, personal communication.
17. The orientation relation between olivine and ilmenite given in the report (*2*) as $[100]_{ol} \parallel [0001]_{ilm}$, $[010]_{ol} \parallel \langle 11\bar{2}0\rangle_{ilm}$, and $[001] \parallel \langle 01\bar{1}0\rangle$ should be written as $[100]_{ol} \parallel [0001]_{ilm}$, $[010]_{ol} \parallel \langle 11\bar{2}0\rangle_{ilm}$, and $[001] \parallel \langle 1\bar{1}00\rangle$.
18. Dynamical diffraction is the exchange of diffracted intensity among all reflections in a pattern. Dynamical diffraction within the olivine structure is present in figure 3, A and B, of the report (*2*), where forbidden olivine reflections occur in both [001] and [100] zone-axis patterns. The $h \neq 2n$ reflections along the h00 row in Fig. 3A and the $k \neq 2n$ reflections along the 0k0 row in Fig. 3B are extinct in the Pbnm structure of olivine due to the *n*-glide on (010) ($h + 1 \neq 2n$ extinctions for all (h0l) reflections) and the b-glide on (100) ($k \neq 2n$ extinctions for all (0kl) reflections).
19. J. W. Edington, in *Practical Electron Microscopy in Materials Science*, N. V. Philips, Ed., (Gloeilampenfabrieken, Einhoven, Germany, 1976), pp. 89–90.
20. There do not appear to be any dynamical effects in figure 3C of the report (*2*), where ilmenite reflections are rediffracted by olivine in the image parallel to the olivine [010] zone axis. The ilmenite 0330 reflection in figure 3C of the report (*2*) is incorrectly indexed as $06\bar{6}0$.
21. P. Y. Simmons, F. Dachille, *Acta Crystallogr.* **23**, 334 (1967); T. Gasparik, *J. Geophys. Res.* **95**, 15,751 (1990); R. E. G. Pacalo and T. Gasparik, *ibid.*, p. 15,853; R. J. Angel, A. Chopelas, N. L. Ross, *Nature* **358**, 322 (1992).
22. First number given for TiO_2 and Cr_2O_3 is bulk, electron-probe value; second number is secondary ion mass spectrometry value for inclusion-free portions of crystals. Olivine, enstatite, diopside, and garnet were analyzed with a JEOL JXA-733 electron microprobe at Stanford University and a Cameca SX-50 at the University of California, Santa Barbara. Major element concentrations were determined with 15 keV accelerating voltage, 2-μm beam diameter, and 15-nA beam current; minor elements, including Ti, were analyzed with the use of 5-, 10-, and 20-μm-diameter beams, 40- to 100-nA beam current, and peak counting times of 200 to 2000 s. Li, V, Cr, and Ti of SL14a olivine were analyzed by secondary ion mass spectrometry with the use of a modified Cameca 3F at Arizona State University operated at a mass resolving power of ~3000 and calibrated against samples described by Hervig *et al.* (*9*). Titanate analyses were made with a Philips CM20 FEG transmission electron microscope at Stanford University operating at 200 keV, nominal spotsize of 2 nm, counting rates of 1000 to 2000 counts per second, counting times of 200 s, and referenced to adjacent olivine of the same thickness. Sample AA8 was collected from Alpe Arami in 1985 by B. R. Hacker.
23. M. Akaogi, E. Ito, A. Navrotsky, *J. Geophys. Res.* **97**, 15,671 (1992).
24. A. Mehta, K. Leinenweber, A. Navrotsky, M. Akaogi, *Phys. Chem. Mineral.* **21**, 207 (1994).
25. G. R. Helffrich, S. Stein, B. J. Wood, *J. Geophys. Res.* **94**, 753 (1989); J. Mercier and A. Nicolas, *J. Petrol.* **16**, 454 (1975).
26. Manuscript was read by W. Bohrson, M. Dalla Torre, W. Gary Ernst, E. Gnos, J. Mosenfelder, and F. Spera. Supported by the NSF.

28 January 1997; revised 6 August 1997; accepted 9 September 1997

Response: We welcome the opportunity to respond to the comment by Hacker *et al.* about our suggestion that the Alpe Arami garnet lherzolite of the Lepontine Alps surfaced from a depth of more than 300 km (*1*). In our report, we described abundant rod-shaped precipitates of $FeTiO_3$ in the older generation of olivine. By image analysis performed on optical micrographs taken in vertically incident reflected light, we measured rod concentrations in large areas of approximately 1% by volume, implying a concentration of TiO_2 in olivine, before exsolution, of ~0.7% by weight (*1*). Rods of $FeTiO_3$ had not been reported in olivine from any environment. A transmission optical micrograph of a region of olivine crystal, in which the rods are viewed edge-on, shows a concentration of $FeTiO_3$ rods of ~1% by volume (Fig. 1A). In our report (*1*), we presented electron diffraction patterns showing that some of the rods are ilmenite, but that other rods exhibited patterns that we interpreted as incompatible with the crystal structure of ilmenite. We suggested that the latter patterns represent a series of metastable phases reflecting the

former presence of the high-pressure, perovskite, polymorph of ilmenite.

On the basis of these observations and others, we concluded that the Alpe Arami massif had experienced physical conditions not previously sampled at the surface of Earth, in which the solubility of TiO_2 in olivine was much higher than that recorded from any previously analyzed olivine (*2*), and that the shape and crystallography of the $FeTiO_3$ precipitates implied that the most likely site of origin was at depths greater than 300 km. Alternatively, we speculated that the phase which originally exhibited high solubility of TiO_2 and trivalent cations such as Al and Cr could have been some other mineral that preceded olivine in the paragenesis. The most likely such phase would be wadsleyite, the high-pressure polymorph of olivine stable in Earth only at depths greater than the 410-km seismic discontinuity, in the mantle transition zone (*3*). Previous work has shown that trivalent cations are highly soluble in wadsleyite (*4*), and our preliminary experiments show that sufficient TiO_2 also can be dissolved in wadsleyite (*5*). Our inference of very high original TiO_2 content of olivine is now questioned by Hacker *et al.* on the basis of broad-beam electron microprobe measurements of TiO_2 in $FeTiO_3$ rod-bearing olivine of similar rocks from an ultrahigh pressure metamorphic terrane in China and specimens of the Alpe Arami peridotite from their own and our collections. They also suggest a different interpretation of our published electron diffraction patterns. We present here further illustration of the abundance and size of $FeTiO_3$ precipitates in Alpe Arami olivine and offer some potential resolutions of the conflicting observations.

Since our report (*1*), we have determined that the abundance and, especially, the size of rods decrease with post-precipitation reactions. Second-generation (recrystallized) olivine is barren of rods, and first generation olivine in specimens that have experienced significant hydrous alteration has fewer and thinner rods. The olivine of our original material has been only weakly "serpentinized," with olivine replacement by hydrous phases ranging from <5% to ~10%. To investigate the correlation of alteration with rod size and abundance, we have made many more measurements (*6*). The distribution of volume fraction of $FeTiO_3$ rods, measured in 125 olivine crystals from 20 thin sections of our original specimens, range from 0.1 to 0.9% by volume (Fig. 1B), with a mean of 0.53 vol%, corresponding to TiO_2 concentrations in olivine before exsolution of the rods of 0.07 to 0.6% TiO_2 by weight. These more extensive measurements confirm our original estimate of the solubility of TiO_2 at about 0.6% by weight, but show that the concentration preserved as precipitates in this original material is variable and in many cases significantly reduced from the maximum.

In more altered specimens of material from this same outcrop (20 to 40% of olivine replaced by serpentine minerals), the abundance and size of rods in olivine is dramatically reduced. A micrograph of a crystal (Fig. 1C) shows one of the more dense concentrations of needle-like rods in such material (micrographs in Fig. 1 are all of the same magnification); a histogram of rod densities measured in such material (Fig. 1D) reveals a mean density of 0.04 v%. The concentrations in Fig. 1D are approximately 10-fold lower than in Fig. 1B; all measurements in Fig. 1D would plot in the smallest bin in Fig. 1B. We tentatively attribute the reduction of size, especially diameter, of the rods in altered rocks to diffusive transfer of $FeTiO_3$ from the rods to ilmenite crystals growing in the grain-boundary and fracture network (Ostwald ripening). Such a diffusion-controlled phenomenon would also be consistent with the observation that some of the rods in olivine of the Bixiling locality of Dabie Shan (*5*) now consist of magnetite (*7*), suggesting that the rods have been changed in composition during low-temperature hydrous alteration by an oxidizing fluid. This profound difference between the density and size of rods in our original material and that occurring in other samples of the Alpe Arami peridotite probably explains why previous workers did not report them, except for one sentence in a paper by Möckel (*8*). Buiskool Toxopeus (*8*), who did an extensive and thorough study at both the optical and transmission electron microscope (TEM) scales, did not report them, probably because the materials he examined had only trivial concentrations of titanate rods.

The reduced abundance and diameter of rods in more altered rocks was discovered during discussions we had with B. Hacker in the fall of 1996. Comparison of his material from the Chijiadian garnet lherzolite in the Sulu region of the Dabie mountains with our original material showed the former to contain similar, but much smaller and less abundant rods. The collection of Hacker *et al.* is also considerably more affected by hydrous alteration (>50% of the olivine has been converted to serpentine minerals) than our freshest rock, which formed the basis of our original arguments (*1, 5*). To pursue the differences between his observations and ours, and to compare his technique of broad-beam electron microprobe

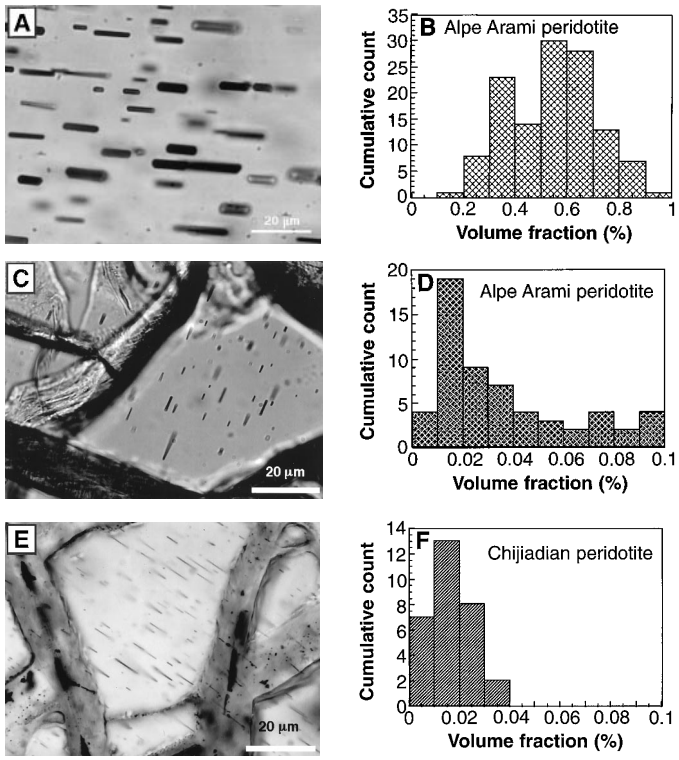

Fig. 1. Photomicrographs and size distributions of $FeTiO_3$ rods in olivine from Alpe Arami garnet lherzolite specimen #73AA3-d (**A** and **B**), Alpe Arami garnet lherzolite specimen #73AA3-26 (**C** and **D**), and Chijiadian garnet peridotite specimen #SL-14 (**E** and **F**). All images (A, C, and E) were obtained at the same conditions in the same Nikon optical photomicroscope in transmitted plain-polarized light, with a 100× objective lens. Accompanying each image is a histogram (B, D, and F) of the volume fraction of rods calculated from measurements of areal fraction in images taken with vertically incident reflected light of olivine crystals with (010) approximately in the plane of the thin section so that the rods were seen end-on. The variation of density and size of the $FeTiO_3$ rods depicted in the images is confirmed by the quantitative measurements. (B) Alpe Arami fresh sample, n = 125 grains of olivine from 20 thin sections, serpentization < 5% to 10%; (D) Alpe Arami altered sample, n = 58 grains of olivine from three thin sections, serpentization = 20% to 40%; (F) Chijiadian peridotite (SL-14, Hacker's collection), n = 30 grains of olivine from one thin section, serpentization ≥ 50%.

analysis with ours of image analysis, we exchanged specimens. For comparison with our Alpe Arami specimens, we show one of the most rod-rich areas in the thin section SL-14 provided to us by Hacker *et al.* (Fig. 1E). The range of volume fractions calculated as before for crystals viewed parallel to [010] is shown (Fig. 1F). The similarity of histograms in Fig. 1, D and F, confirms the similarity of images in Fig. 1, C and E. As for Fig. 1D, the entire range of measurements in Fig. 1F would plot in the lowest bin of Fig. 1B. Calculation of TiO_2 contents from these measurements (Table 1) is in good agreement with the data of Hacker *et al.* from broad-beam electron microprobe measurements.

Hacker *et al.* also performed image analysis on several of our micrographs and confirmed our estimation of tenths of percent volume fraction rods in those crystals (Table 1) in contrast to the much lower fraction they infer from their probe analysis. The rod diameters and abundances in Fig. 1 confirm that the volume of titanate in fresh Alpe Arami olivine exceeds that of the more altered specimens by more than a factor of 10; the bulk TiO_2 content of the material of Fig. 1A can be the same as that of Fig. 1, C and E, only if the rods of Fig. 1A are deficient in TiO_2 by a similar factor. This contradiction between techniques is most likely attributable to the well-known observation that multiple-phase analysis by electron microprobe is subject to significant errors (*9*).

The crystallographic arguments of Hacker *et al.* are correct insofar as they go. Ilmenite and olivine have the same basic hcp oxygen sublattice, thus many of their corresponding d-spacings are similar. Also, multiple diffraction between olivine and ilmenite could produce the extra spots observed in Fig. 3, A and B, of our report (*1*). The same would be true if the rods are composed of the lithium niobate crystal structure which is the usual quench product of the $FeTiO_3$ perovskite structure (*10*). It is difficult to distinguish between lithium niobate and ilmenite structures by selected area electron diffraction in cases where multiple diffraction effects take place; the only low-index zone axis diffraction patterns definitively showing the difference are $<11\bar{2}0>$. However, if the extra spots in our diffraction patterns are satellites produced by multiple diffraction from either the ilmenite or lithium niobate structure, one would also expect other satellite spots that are not observed in figure 3, A and B, of our report (*1*). The other diffraction patterns in our collection also do not show the predicted additional spots. Because all of the rods should have inverted to ilmenite and at least some of them have done so [for example, figure 3C in (*1*)], we leave resolution of this problem to future work. However, if the rods are all ilmenite, their TiO_2 contents are fixed, and the difference in volumetric proportion of rods in Fig. 1, A and B, as opposed to those of Fig. 1, C to F, translates directly into a similar difference in TiO_2 content. Thus, we are led back to our original conclusion that the Alpe Arami massif contains olivine which previously exhibited TiO_2 solubility of order 0.6% by weight.

The comment by Hacker *et al.*, our report of $FeTiO_3$ rods from Dabie Shan peridotites (*5*), and a report of other peridotites in the same Alpine nappe as Alpe Arami (*11*) show that Alpe Arami is not unique in displaying these precipitates. All of these observations involve subduction-zone garnet peridotites, supporting our original suggestion that a previously unrecognized unusual mantle environment is being sampled. The possibility remains that this is a very high-pressure environment, but if an ultradeep origin for Alpe Arami is rejected, an alternative explanation must be found for the family of observations on which we built our original hypothesis (*1*). Critical to this discussion are the observations that: (i) the great abundance of $FeTiO_3$ and spinel precipitates in first-generation olivine in Alpe Arami have no known counterpart in any other peridotite massif or xenolith; (ii) the precipitates are older than all minerals and microstructures that can be definitely attributed to the Alpine metamorphism (*5*); and (iii) the precipitates predate the dislocation microstructure present in both generations of olivine, the recrystallization that accompanied development of that dislocation microstructure, and all hydrous alteration of the original assemblage (*5*). The evidence collected so far is consistent with rod precipitation occurring before the maximum conditions of metamorphism recorded by standard thermobarometric analysis.

Table 1. Measurements of volume fraction of $FeTiO_3$ rods

Sample/image numbers	Our measurements (volume %)	Measurements by Hacker *et al.* (*18*) (volume %)
Alpe Arami #73AA3		
ol-1 rBSEx400	0.42	0.5
ol-1 lBSEx400	0.57	0.7–1.0
ol-1 BSEx100	*	0.5
ol-2 BSEx400	0.10	No data
ol-2 lBSEx500	0.63	0.7–1.0
ol-2 rBSEx500	0.12	0.1–0.2
ol-3 BSEx500	0.52	0.4–0.7
Chijiadian #SL-14	0.016	No data

*Rod size at this magnification is below the sensitivity of analysis by NIH Image.

Last, if the solubility of TiO_2 in the olivine was not higher than commonly found in olivine, as stated by Hacker *et al.*, then why would the precipitates form in the first place?

One alternative possibility to our great-depth scenario would be that in a hydrous environment at moderate temperature and high pressure, the solubility of TiO_2 and trivalent cations in olivine may be significantly greater than under dry conditions. Such environments are not represented by xenoliths from diamond pipes (which show no rods and TiO_2 contents of a few hundred parts per million), but could be sampled by subduction to perhaps 150 km and return to the surface. Thus, in a mantle-wedge environment just above a downgoing slab, hydrous fluids (melts?) emanating from the slab could metasomatize mantle peridotite and perhaps significant TiO_2 could be dissolved in olivine, along with elevated concentrations of Al_2O_3 and Cr_2O_3. Subsequent dehydration of such material perhaps could precipitate $FeTiO_3$ + chromite in the quantities observed (*1*, *5*). The ultimate explanation must take into account all of these observations, including the restriction to subduction-zone garnet peridotites and the fact that rod precipitation occurred early in the recorded history of the rocks.

In a detailed review of the geochemical and geochronological data about Alpe Arami, Brenker and Brey (*12*) show that the *minimum* conditions of origin of this massif are 5 GPa (160 km), 1400 K, at 35 to 40 million years ago. This is the limit of *chemical* memory in these rocks because it corresponds to diffusive closure of the most sluggish reactions in the peridotite system. The *microstructural* memory preserved as precipitates in olivine and the spatial association of diopside and garnet (*1*, *5*), however, extends back further and implies greater depths. Whether the additional depth of origin is hundreds of kilometers or only a few tens of kilometers remains an open question. Our preliminary experiments (*5*) suggested that at 6 GPa, 1700 K, solubility of TiO_2 in olivine was still too low to explain our observations. More recent work confirms these results to 8 GPa, 1600 K, but suggests that solubility of TiO_2 may increase sufficently at 12 GPa (*13*). Our experimental program will continue to test both the very high pressure and hydrous environment hypotheses.

Finally, we agree with Hacker *et al.* that specific supporting observations of preserved high-pressure phases would strengthen our hypothesis of an ultrahigh-pressure origin of the Alpe Arami massif. They mention, as one of the candidate phases, the high-pressure polymorph of clinoenstatite.

Of possible great significance in this regard, clinoenstatite lamellae have been found in diopside from Alpe Arami (*14*). To our knowledge, this is the only occurrence of clinoenstatite in diopside recorded. A possible explanation would be exsolution of high-pressure clinoenstatite from diopside at very high pressures [$P > 8$ GPa for a normal mantle geotherm (*15*)] and inhibition of transformation to orthoenstatite during subsequent pressure reduction because of sluggish nucleation kinetics or coherency stresses between the lamellae and diopside host. The high-pressure polymorph of clinoenstatite cannot be preserved because at lower pressures it undergoes a nonquenchable second-order transformation to the low pressure form (*16*). Nevertheless, if clinoenstatite could be found again in diopside of these rocks, it could be examined for the possible presence of the diagnostic antiphase boundaries that would confirm the previous existence of the high-pressure polymorph.

Harry W. Green, II
Larissa Dobrzhinetskaya
Krassimir Bozhilov
Institute of Geophysics and Planetary Physics and *Department of Earth Sciences, University of California, Riverside, CA 92521, USA*
E-mail: hgreen@ucrac1.ucr.edu

REFERENCES AND NOTES

1. L. F. Dobrzhinetskaya, H. W. Green II, S. Wang, *Science* **271**, 1841 (1996).
2. R. L. Hervig, J. V. Smith, J. B. Dawson, *R. Soc. Edinburgh Trans. Earth Sci.* **77**, 181 (1986).
3. The mantle transition zone occurs between the prominent seismic discontinuities at depths of 410 and 660 km (P = 13 to 24 GPa); wadsleyite is not stable at pressures less than ~12 GPa.
4. T. E. Young, H. W. Green II, A. Hofmeister, D. Walker, *Phys. Chem. Miner.* **19**, 409 (1993); C. Dupas, N. Doukhan, J.-C. Doukhan, H. W. Green II, T. E. Young, *J. Geophys. Res.* **99**, 15821 (1994).
5. H. W. Green II, L. F. Dobrzhinetskaya, E. Riggs, Z.-M. Jin, *Tectonophysics*, in press.
6. We have restricted these new measurements to crystals in which [010] lies approximately perpendicular to the plane of the thin section, thus the rods are seen as end sections. Measurements were analyzed with the use of the program NIH Image (National Institutes of Health, Bethesda, MD) for Macintosh; areas were always chosen for measurement such that the total area was large compared to precipitate size and spacing. The only assumption necessary to convert areal fractions measured in reflection in the optical microscope or in the scanning electron microscope (SEM) to volume fraction is that all cross sections are statistically the same. For end-section views, this is a good approximation, whereas for other observations any tendency for the rods to lie in planes could bias the measurements. For the specific case of the differences between ourselves and Hacker *et al.*, the only assumption necessary is that the rods extend below the surface more than the penetration distance of the electron beam of their analyses. For the small number of rods which might penetrate less, it is equally probable that additional rods lie just below the surface.
7. Z. M. Jin, personal communication.
8. J. R. Möckel, *Leidse Geol. Med.* **42**, 61 (1969); J. M. A. Buiskool Toxopeus, *ibid.* **51**, 1 (1976); *N. Jb. Miner. Abh.* **129**, 233 (1977); *Tectonophys.* **39**, 55 (1977).
9. Implicit in the approach of Hacker *et al.* is that bulk analysis of the composite olivine + $FeTiO_3$ gives accurate results. However, it is common practice in electron probe microanalysis to go to great lengths to independently analyze all phases separately in order to avoid serious analytical errors. For example, J. I. Goldstein *et al.* [*Scanning Electron Microscopy and X-ray Microanalysis* (Plenum, New York, ed. 3, 1992)] strongly caution against attempting such bulk analysis. They state (p. 415), "Note that this requirement for specimen homogeneity within the analyzed volume eliminates the use of overscanning a field of view containing multiple phases during spectrum accumulation to get an average analysis. Such a procedure can lead to relative errors of hundreds of percent!"
10. K. Leinenweber, W. Utsumi, Y. Tsuchida, T. Yagi, K. Kurita, *Phys. Chem. Minerals* **18**, 244 (1991).
11. A. C. Risold, V. Trommsdorff, E. Reusser, P. Ulmer, B. Grobety, *Eos* **77**, F761 (1996); A. C. Risold, V. Trommsdorff, E. Reusser, P. Ulmer, M. Pfiffner, *Europ. Geophys. Union* **9**, 93 (1997).
12. F. E. Brenker and G. P. Brey, *J. Metamorphic Geol.*, in press.
13. L. Dobrzhinetskaya and H. W. Green II, *Eos*, in press.
14. Y. Yamaguchi, J. Akai, K. Tomita, *Contrib. Mineral. Petrol.* **66**, 263 (1978).
15. R. E. G. Pacalo and T. Gasparik, *J. Geophys. Res.* **95**, 15853 (1990).
16. R. J. Angel, A. Chopelas, N. L. Ross, *Nature* **358**, 322 (1992).
17. We thank E. Riggs and an anonymous reviewer for helpful comments which led to clarification of our presentation. Supported by National Science Foundation grant EAR96-283432.
18. B. R. Hacker *et al.*, personal communication of December 1996.

8 May 1997; revised 8 September 1997; accepted 9 September 1997